Ultrasound
in medicine
and biology

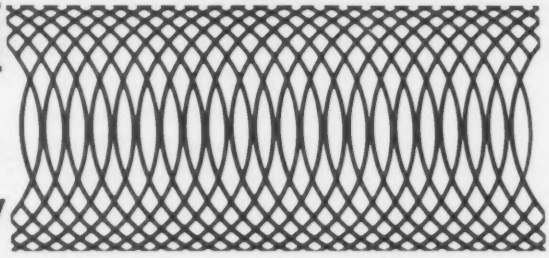

Supplement to *Ultrasound in Medicine and Biology*, Volume 19, Number 4, 1993

Author–Subject Index
Volume 18 (1992)

Compiled by

Michael Halliwell
Department of Medical Physics, Bristol General Hospital, Bristol BS1 6SY, United Kingdom

PERGAMON PRESS

NEW YORK · OXFORD · SEOUL · TOKYO

ULTRASOUND IN MEDICINE AND BIOLOGY

WORLD FEDERATION FOR ULTRASOUND IN MEDICINE AND BIOLOGY

President: M. FUKUDA, *Sapporo, Japan*
Vice-President: H. TAKEUCHI, *Tokyo, Japan*
Past-President: F. WEILL, *Besançon, France*
President-Elect: B. GOLDBERG, *Philadelphia, USA*
Treasurer: W. O'BRIEN, *Urbana, USA*
Secretary: D. ROBINSON, *Chatswood, Australia*
Editor-in-Chief of the Journal: P. N. T. WELLS, *Bristol, UK*
Councillors: C. R. B. MERRITT, *New Orleans, USA*
H. WATANABE, *Kyoto, Japan*
H. LUTZ, *Bayreuth, Germany*
G. CERRI, *São Paulo, Brazil*
W. WIBISONO, *Jakarta, Indonesia*
S. HANCKE, *Hellerup, Denmark*
M. ZISKIN, *Philadelphia, USA*
S. EIK-NES, *Trondheim, Norway*

AFFILIATED SOCIETIES

American Institute of Ultrasound in Medicine (AIUM), L. Nelson, Secretary, 11200 Rockville Pike, Suite 205, Rockville, MD 20852-3139, USA

Asian Federation of Societies for Ultrasound in Medicine and Biology (AFSUMB), Dr. H. Watanabe, Secretary, Dept. of Urology, Kyoto Prefectural University of Medicine, Kawaramachi-Hirokoji, Kyoto, Japan 602

Australasian Society for Ultrasound in Medicine (ASUM), Secretariat ASUM, 126 Greville Street, Chatswood, NSW 2067, Australia

Egyptian Society for Ultrasonics (ESU), Dr. Y. Mohran, Secretary, 376 Pyramids Road, Giza, Cairo, Egypt

European Federation of Societies for Ultrasound in Medicine and Biology (EFSUMB), Mrs. Lee Surry, Executive Secretary, The Studio, 43 Bond Street, Ealing, London, WS 5AS, UK

Latin-American Federation of Societies of Ultrasound in Medicine and Biology (LAFSUMB), Dr. Giovanni Guido Cerri, Av. Paulista, 491 13.° conj. 132, CEP 01311, São Paulo, Brazil

Mediterrean Society of Ultrasonic Societies (MASU), Dr. F. Weill, Secretary, Centre Hospitalier et Universitaire de Besançon, 2 Place Saint-Jaques, 25030 Besançon Cedex, France

Societas Internationalis pro Diagnostica Ultrasonica in Ophthalmologia (SIDUO), Dr. J. M. Thijssen, Secretary, Universiteitskliniek voor Oogheelkunde, 6500 HB Nijmegen, The Netherlands

South African Medical Ultrasound Society (SAMUS), Dr. M. Jacobson, Secretary SAMUS, Box 93499, Yeoville 2143, Republic of South Africa

Production Editor: L. Johnson, Pergamon Press, Tarrytown, New York.

Publishing, Advertising, and Subscription Offices: Pergamon Press Inc., 660 White Plains Road, Tarrytown, NY 10591-5153, USA, INTERNET "PPI@PERGAMON.COM"; or Pergamon Press Ltd., Headington Hill Hall, Oxford OX3 0BW, United Kingdom.

Published 9 per Annum. *Annual Institutional Subscription Rate* (1993): £315.00 (US $504.00). Sterling prices are definitive. US dollar prices are quoted for convenience only, and are subject to exchange rate fluctuation. Prices include postage and insurance and are subject to change without notice. Members of the World Federation for Ultrasound in Medicine and Biology may order personal subscriptions at a concessional rate; details of these rates are available upon request.

Copyright © 1993 Pergamon Press Ltd.

The Item-Fee Code for this publication is: 0301-5629/93 $6.00 + .00

Ultrasound in Med. & Biol. Vol. 19, Suppl., pp. 3–44, 1993
Printed in the USA

0301–5629/93 $6.00 + .00
© 1993 Pergamon Press Ltd.

AUTHOR/SUBJECT INDEX

A

Abdominal aorta
noninvasive measurement of diameter changes in the distal abdominal aorta in man (Länne), 451

Ablation
computer model of ultrasonic hyperthermia and ablation for ocular tumors using B-mode data (Lizzi), 59

Abraham, V., see Margulies, N.

Absorption
digital path-dependent recompensation of contrast-enhanced echocardiographic images (Mor-Avi), 831

Acousto-electrical effect
ultrasonic vibrational potentials in gels and preparations of biological tissue (Rosenfeld), 607

Adamson, S. L. and Langille, B. L.: factors determining aortic and umbilical blood flow pulsatility in fetal sheep, 255

Adaptive processing
adaptive time gain compensation for ultrasonic imaging (Pye), 205

Adriamycin
ultrasound-enhanced effects of adriamycin against murine tumors (Saad), 715

Ageing
simultaneous cardio-cerebral ultrasonic measurement technique for assessing the interrelationship between cardiac and cerebral circulations in elderly subjects: a preliminary study (Matsumoto), 45

Akashi, K., see Makinaga, G.

Akselrod, S., see Mor-Avi, V.

Alanen, A., see Bondestam, S.

Alder, R. S., Dedrick, D. K., Laing, T. J., Chiang, E. H., Meyer, C. R., Bland, P. H. and Rubin, J. M.: quantitative assessment of cartilage surface roughness in osteoarthritis using high frequency ultrasound, 51

Alexander, K., see Ranke, C.

Aliasing
visualization of complex flow fields, with application to the interpretation of colour flow Doppler images (Vera), 1

Anastomoses
visualization of complex flow fields, with application to the interpretation of colour flow Doppler images (Vera), 1

Anatomy
identifying acoustic scattering sources in normal renal parenchyma *in vivo* by varying arterial and ureteral pressures (Insana), 587

Angiography
duplex scanning of the peripheral arteries: correlation of the peak velocity ratio with angiographic diameter reduction (Ranke), 433

Angioplasty
how useful are acceleration- and deceleration-based Doppler indices? A trial on patients with percutaneous transluminal angioplasty (Windeck), 525

Anterior cerebral artery
cerebral blood flow velocity: the influence of myocardial contractility on the velocity waveform of brain supplying arteries (Van Bel), 441

continuous and simultaneous ultrasound Doppler velocity of the internal carotid and vertebral arteries: preliminary observations of cerebral blood flow changes with common carotid compression (Makinaga), 637

new implanted Doppler sensors for the assessment of the main fetal hemodynamics (Arbeille), 97

reproducibility of transcranial Dopplersonography: a validation study (Totaro), 173

ultrasound Doppler spectral analysis in the diagnosis of occlusive lesions of the carotid arteries (Cooperberg), 421

Aorta
factors determining aortic and umbilical blood flow pulsatility in fetal sheep (Adamson), 255

noninvasive measurement of diameter changes in the distal abdominal aorta in man (Länne), 451

pulse pressure assessment in the human fetal descending aorta (Struijk), 39

Aortic diameter
noninvasive measurement of diameter changes in the distal abdominal aorta in man (Länne), 451

Arbeille, Ph., Berson, M., Maulik, D., Locatelli, A. and Bodard, S.: new implanted Doppler sensors for the assessment of the main fetal hemodynamics, 97

Arterial blood pressure
noninvasive measurement of diameter changes in the distal abdominal aorta in man (Länne), 451

Arterial diameter
noninvasive measurement of diameter changes in the distal abdominal aorta in man (Länne), 451

pulse pressure assessment in the human fetal descending aorta (Struijk), 39

Arterioventricular valves
reproducibility of fetal cardiac flow velocity waveforms at atrioventricular level (van der Mooren), 827

Artery
cerebral blood flow velocity: the influence of myocardial contractility on the velocity waveform of brain supplying arteries (Van Bel), 441

color Doppler characteristics in normal lower extremity arteries (Hatsukami), 167

comparison of flow disturbances in small carotid atheroma using a multi-gate pulsed Doppler system and Doppler color flow imaging (Steinke), 11

duplex scanning of the peripheral arteries: correlation of the peak velocity ratio with angiographic diameter reduction (Ranke), 433

factors determining aortic and umbilical blood flow pulsatility in fetal sheep (Adamson), 255

how useful are acceleration- and deceleration-based Doppler indices? A trial on patients with percutaneous transluminal angioplasty (Windeck), 525

modelling the feto-placental circulation: 1. A distributed network predicting umbilical haemodynamics throughout pregnancy (Guiot), 535

modelling the feto-placental circulation: 2. A continuous approach to explain normal and abnormal flow velocity waveforms in the umbilical arteries (Todros), 545

new implanted Doppler sensors for the assessment of the main fetal hemodynamics (Arbeille), 97

noninvasive measurement of diameter changes in the distal abdominal aorta in man (Länne), 451

pulse pressure assessment in the human fetal descending aorta (Struijk), 39

quantification of Doppler color flow images from a stenosed carotid artery model (Vattyam), 195

reproducibility of transcranial Dopplersonography: a validation study (Totaro), 173

simultaneous cardio-cerebral ultrasonic measurement technique for assessing the interrelationship between cardiac and cerebral circulations in elderly subjects: a preliminary study (Matsumoto), 45

the assessment of benign uterine tumor vascularization by transvaginal color Doppler (Kurjak), 645

ultrasound Doppler spectral analysis in the diagnosis of occlusive lesions of the carotid arteries (Cooperberg), 421

ultrasound-enhanced effects of adriamycin against murine tumors (Saad), 715

vector Doppler: accurate measurement of blood velocity in two dimensions (Overbeck), 19

Articular cartilage roughness
quantitative assessment of cartilage surface roughness in osteoarthritis using high frequency ultrasound (Awer), 51

Atherosclerosis
comparison of flow disturbances in small carotid atheroma using a multi-gate pulsed Doppler system and Doppler color flow imaging (Steinke), 11

quantification of Doppler color flow images from a stenosed carotid artery model (Vattyam), 195

ultrasound Doppler spectral analysis in the diagnosis of occlusive lesions of the carotid arteries (Cooperberg), 421

Attenuation
a comparison of theoretical and experimental ultrasound field distributions in canine muscle tissue *in vivo* (Moros), 81

correction of diffraction errors in attenuation estimation with dynamic beam translation (Céspedes), 213

dependence of ultrasonic attenuation of liver on pathologic fat and fibrosis: examination with experimental fatty liver and liver fibrosis models (Suzuki), 657

digital path-dependent recompensation of contrast-enhanced echocardiographic images (Mor-Avi), 831

fetal exposure from endovaginal ultrasound examinations in the first trimester (Hussain), 675

human *in situ* dosimetry: differential insertion loss during passage through abdominal wall and myometrium (Siddiqi), 681

in vitro classification of gallstones by quantitative echography (Goedegebure), 553

sonic velocity and attenuation in wet compact cow femur for the frequency range 5 to 100 MHz (Lees), 303

Autoregressive technique
simulation of Doppler ultrasound signals for a laminar, pulsatile, nonuniform flow (Wendling), 179

Axial beam translation
correction of diffraction errors in attenuation estimation with dynamic beam translation (Céspedes), 213

B

B-mode imaging
adaptive time gain compensation for ultrasonic imaging (Pye), 205

computer model of ultrasonic hyperthermia and ablation for ocular tumors using B-mode data (Lizzi), 59

high-resolution real-time ultrasonic scanner (Berson), 471

in vitro classification of gallstones by quantitative echography (Goedegebure), 553

Baan, J., see Van Bel, F.

Backscatter
a method for computer simulation of ultrasound Doppler color flow images. I. Theory and numerical method (Kerr), 861

a velocity evaluation phantom for colour and pulsed Doppler instruments (Rickey), 479

cellularity and fibrin mesh properties as a basis for ultrasonic tissue characterization of blood clots and thrombi (Loiacono), 399

correlations of liver echo intensity with cytology and chemical measurements of fat, water and protein content in live burbots (*Lota lota*) (Bondestam), 75

differentiation of normal and ischemic right ventricular myocardium with quantitative two-dimensional integrated backscatter imaging (Waggoner), 249

digital path-dependent recompensation of contrast-enhanced echocardiographic images (Mor-Avi), 831

identifying acoustic scattering sources in normal renal parenchyma *in vivo* by varying arterial and ureteral pressures (Insana), 587

in vitro classification of gallstones by quantitative echography (Goedegebure), 553

new method of estimating the ultrasonic beam ratio parameter for characterizing sound propagation in tissue (Fein), 881

quantitative assessment of cartilage surface roughness in osteoarthritis using high frequency ultrasound (Alder), 51

red cell aggregation and the echogenicity of whole blood (Mahony), 579

the effect of heparin versus citrate on blood echogenicity *in vitro:* the role of platelet and platelet-neutrophil aggregates (Mahony), 851

Bactericidal activity

conservation of bactericidal activity in ultrasound-exposed murine peritoneal phagocytic cells (Prohaska), 601

Basilar artery

reproducibility of transcranial Dopplersonography: a validation study (Totaro), 173

Beach, K. W., see Overbeck, J. R.

Beach, K. W.: 1975–2000: a quarter century of ultrasound technology, 377

Beam distortion

a comparison of theoretical and experimental ultrasound field distributions in canine muscle tissue *in vivo* (Moros), 81

the early development of neurosonology. I. Echoencephalography in adults (White), 115

Beam plotting

a comparison of theoretical and experimental ultrasound field distributions in canine muscle tissue *in vivo* (Moros), 81

correction of diffraction errors in attenuation estimation with dynamic beam translation (Céspedes), 213

new method of estimating the ultrasonic beam ratio parameter for characterizing sound propagation in tissue (Fein), 881

temperature rise in a tissue-mimicking material generated by unfocused and focused ultrasonic transducers (Wu), 495

the early development of neurosonology. I. Echoencephalography in adults (White), 115

Beam profile

a comparison of theoretical and experimental ultrasound field distributions in canine muscle tissue *in vivo* (Moros), 81

correction of diffraction errors in attenuation estimation with dynamic beam translation (Céspedes), 213

new method of estimating the ultrasonic beam ratio parameter for characterizing sound propagation in tissue (Fein), 881

temperature rise generated by a focussed Gaussian beam in a two-layer medium (Wu), 293

Beam ratio parameter

new method of estimating the ultrasonic beam ratio parameter for characterizing sound propagation in tissue (Fein), 881

Beam tracking

on the feasibility of pulse-echo speed of sound estimation in small regions: simulation studies (Céspedes), 283

Bengtsson, H., see Länne, T.

Bergqvist, D., see Länne, T.

Berson, M., see Arbeille, Ph.

Berson, M., Vaillant, L., Patat, F. and Pourcelot, L.: high-resolution real-time ultrasonic scanner, 471

Bioeffects

apparent contribution of respiratory gas exchange to the *in vitro* "cell density effect" in ultrasonic cell lysis (Brayman), 701

bubble cycling and standing waves in ultrasonic cell lysis (Brayman), 411

computed estimates of maximum temperature elevations in fetal tissues during transabdominal pulsed Doppler examinations (Bly), 389

computer model of ultrasonic hyperthermia and ablation for ocular tumors using B-mode data (Lizzi), 59

conservation of bactericidal activity in ultrasound-exposed murine peritoneal phagocytic cells (Prohaska), 601

effect of ultrasound on the neonatal rat brain (Margulies), 459

influence of dissolved and free gases on iodine release and cell killing by shock waves *in vitro* (Gambihler), 617

in vitro investigations on cellular damage induced by high energy shock waves (Steinbach), 691

modest enhancement of ultrasound-induced mutations in V79 cells *in vitro* (Doida), 465

temperature rise generated by a focussed Gaussian beam in a two-layer medium (Wu), 293

the sensitivity of *Drosophila* larvae to continuous-wave ultrasound (Child), 725

ultrasonic vibrational potentials in gels and preparations of biological tissue (Rosenfeld), 607

ultrasound-enhanced effects of adriamycin against murine tumors (Saad), 715

Bland, P. H., see Alder, R. S.

Blood

red cell aggregation and the echogenicity of whole blood (Mahony), 579

the effect of heparin versus citrate on blood echogenicity *in vitro:* the role of platelet and platelet-neutrophil aggregates (Mahony), 851

Blood clots

cellularity and fibrin mesh properties as a basis for ultrasonic tissue characterization of blood clots and thrombi (Loiacono), 399

Blood flow

a method for computer simulation of ultrasound Doppler color flow images—I. Theory and numerical method (Kerr), 861

a method for computer simulation of ultrasound Doppler color flow images—II. Simulation results (Kerr), 873

a velocity evaluation phantom for colour and pulsed Doppler instruments (Rickey), 479

cerebral blood flow velocity: the influence of myocardial contractility on the velocity waveform of brain supplying arteries (Van Bel), 441

color Doppler characteristics in normal lower extremity arteries (Hatsukami), 167

comparison of flow disturbances in small carotid atheroma using a multi-gate pulsed Doppler system and Doppler color flow imaging (Steinke), 11

continuous and simultaneous ultrasound Doppler velocity of the internal carotid and vertebral arteries: preliminary observations of cerebral blood flow changes with common carotid compression (Makinaga), 637

duplex scanning of the peripheral arteries: correlation of the peak velocity ratio with angiographic diameter reduction (Ranke), 433

factors determining aortic and umbilical blood flow pulsatility in fetal sheep (Adamson), 255

modelling the feto-placental circulation: 1. A distributed network predicting umbilical haemodynamics throughout pregnancy (Guiot), 535

modelling the feto-placental circulation: 2. A continuous approach to explain normal and abnormal flow velocity waveforms in the umbilical arteries (Todros), 545

new implanted Doppler sensors for the assessment of the main fetal hemodynamics (Arbeille), 97

quantification of Doppler color flow images from a stenosed carotid artery model (Vattyam), 195

reproducibility of fetal cardiac flow velocity waveforms at atrioventricular level (van der Mooren), 827

reproducibility of transcranial Dopplersonography: a validation study (Totaro), 173

simultaneous cardio-cerebral ultrasonic measurement technique for assessing the interrelationship between cardiac and cerebral circulations in elderly subjects: a preliminary study (Matsumoto), 45

the assessment of benign uterine tumor vascularization by transvaginal color Doppler (Kurjak), 645

vector Doppler: accurate measurement of blood velocity in two dimensions (Overbeck), 19

visualization of complex flow fields, with application to the interpretation of colour flow Doppler images (Vera), 1

Blood velocity

a method for computer simulation of ultrasound Doppler color flow images—I. Theory and numerical method (Kerr), 861

a method for computer simulation of ultrasound Doppler color flow images—II. Simulation results (Kerr), 873

a velocity evaluation phantom for colour and pulsed Doppler instruments (Rickey), 479

cerebral blood flow velocity: the influence of myocardial contractility on the velocity waveform of brain supplying arteries (Van Bel), 441

color Doppler characteristics in normal lower extremity arteries (Hatsukami), 167

continuous and simultaneous ultrasound Doppler velocity of the internal carotid and vertebral arteries: preliminary observations of cerebral blood flow changes with common carotid compression (Makinaga), 637

duplex scanning of the peripheral arteries: correlation of the peak velocity ratio with angiographic diameter reduction (Ranke), 433

factors determining aortic and umbilical blood flow pulsatility in fetal sheep (Adamson), 255

how useful are acceleration- and deceleration-based Doppler indices? A trial on patients with percutaneous transluminal angioplasty (Windeck), 525

reproducibility of fetal cardiac flow velocity waveforms at atrioventricular level (van der Mooren), 827

reproducibility of transcranial Dopplersonography: a validation study (Totaro), 173

Bly, S. H. P., Vlahovich, S., Mabee, P. R. and Hussey, R. G.: computed estimates of maximum temperature elevations in fetal tissues during transabdominal pulsed Doppler examinations, 389

Bodard, S., see Arbeille, Ph.

Bondestam, S., Alanen, A. and Toikkanen, S.: correlations of liver echo intensity with cytology and chemical measurements of fat, water and protein content in live burbots (*Lota lota*), 75

Bone

sonic velocity and attenuation in wet compact cow femur for the frequency range 5 to 100 MHz (Lees), 303

BPD

the early development of neurosonology: II. Fetal and neonatal echoencephalography (White), 227

Brayman, A. A., see Doida, Y.
Brayman, A. A. and Miller, M. W.: bubble cycling and standing waves in ultrasonic cell lysis, 411
Brayman, A. A., Doida, Y. and Miller, M. W.: apparent contribution of respiratory gas exchange to the *in vitro* "cell density effect" in ultrasonic cell lysis, 701

Breast
architectural distortion of subcutaneous fascial layer in breast tumors: ultrasonographic evaluation (Nishimura), 815

Bubbles
bubble cycling and standing waves in ultrasonic cell lysis (Brayman), 411
influence of dissolved and free gases on iodine release and cell killing by shock waves *in vitro* (Gambihler), 617
the sensitivity of *Drosophila* larvae to continuous-wave ultrasound (Child), 725

Burbot
correlations of liver echo intensity with cytology and chemical measurements of fat, water and protein content in live burbots (*Lota lota*) (Bondestam), 75
Burghouwt, M. and Wladimiroff, J. W.: modulation of middle cerebral artery flow velocity waveforms by breathing movements in the normal term fetus, 821

C

Calibration
a method for computer simulation of ultrasound Doppler color flow images—II. Simulation results (Kerr), 873
the influence of spatial polarization distribution on spot pooled PVDF membrane hydrophone performance (Fay), 625

Canine muscle
a comparison of theoretical and experimental ultrasound field distributions in canine muscle tissue *in vivo* (Moros), 81
Cannarsa, C., see Totaro, R.

Cardiac output
reproducibility of fetal cardiac flow velocity waveforms at atrioventricular level (van der Mooren), 827
simultaneous cardio-cerebral ultrasonic measurement technique for assessing the interrelationship between cardiac and cerebral circulations in elderly subjects: a preliminary study (Matsumoto), 45

Carotid
comparison of flow disturbances in small carotid atheroma using a multi-gate pulsed Doppler system and Doppler color flow imaging (Steinke), 11
continuous and simultaneous ultrasound Doppler velocity of the internal carotid and vertebral arteries: preliminary observations of cerebral blood flow changes with common carotid compression (Makinaga), 637

quantification of Doppler color flow images from a stenosed carotid artery model (Vattyam), 195

simultaneous cardio-cerebral ultrasonic measurement technique for assessing the interrelationship between cardiac and cerebral circulations in elderly subjects: a preliminary study (Matsumoto), 45

ultrasound Doppler spectral analysis in the diagnosis of occlusive lesions of the carotid arteries (Cooperberg), 421

vector Doppler: accurate measurement of blood velocity in two dimensions (Overbeck), 19

Carotid volume flow

simultaneous cardio-cerebral ultrasonic measurement technique for assessing the interrelationship between cardiac and cerebral circulations in elderly subjects: a preliminary study (Matsumoto), 45

Carstensen, E. L., see Child, S. Z.

Cartilage

quantitative assessment of cartilage surface roughness in osteoarthritis using high frequency ultrasound (Alder), 51

Cavitation

acoustic emission and sonoluminescence due to cavitation at the beam focus of an electrohydraulic shock wave lithotripter (Coleman), 267

bubble cycling and standing waves in ultrasonic cell lysis (Brayman), 411

modest enhancement of ultrasound-induced mutations in V79 cells *in vitro* (Doida), 465

influence of dissolved and free gases on iodine release and cell killing by shock waves *in vitro* (Gambihler), 617

in vitro investigations on cellular damage induced by high energy shock waves (Steinbach), 691

the sensitivity of *Drosophila* larvae to continuous-wave ultrasound (Child), 725

ultrasonic vibrational potentials in gels and preparations of biological tissue (Rosenfeld), 607

Cells

apparent contribution of respiratory gas exchange to the *in vitro* "cell density effect" in ultrasonic cell lysis (Brayman), 701

bubble cycling and standing waves in ultrasonic cell lysis (Brayman), 411

conservation of bactericidal activity in ultrasound-exposed murine peritoneal phagocytic cells (Prohaska), 601

influence of dissolved and free gases on iodine release and cell killing by shock waves *in vitro* (Gambihler), 617

in vitro investigations on cellular damage induced by high energy shock waves (Steinbach), 691

modest enhancement of ultrasound-induced mutations in V79 cells *in vitro* (Doida), 465

red cell aggregation and the echogenicity of whole blood (Mahony), 579

Cell lysis
apparent contribution of respiratory gas exchange to the *in vitro* "cell density effect" in ultrasonic cell lysis (Brayman), 701

bubble cycling and standing waves in ultrasonic cell lysis (Brayman), 411

Cerebral arteries
cerebral blood flow velocity: the influence of myocardial contractility on the velocity waveform of brain supplying arteries (Van Bel), 441

continuous and simultaneous ultrasound Doppler velocity of the internal carotid and vertebral arteries: preliminary observations of cerebral blood flow changes with common carotid compression (Makinaga), 637

new implanted Doppler sensors for the assessment of the main fetal hemodynamics (Arbeille), 97

reproducibility of transcranial Dopplersonography: a validation study (Totaro), 173

ultrasound Doppler spectral analysis in the diagnosis of occlusive lesions of the carotid arteries (Cooperberg), 421

Cerebral arteriography
ultrasound Doppler spectral analysis in the diagnosis of occlusive lesions of the carotid arteries (Cooperberg), 421

Cerebral flow
cerebral blood flow velocity: the influence of myocardial contractility on the velocity waveform of brain supplying arteries (Van Bel), 441

continuous and simultaneous ultrasound Doppler velocity of the internal carotid and vertebral arteries: preliminary observations of cerebral blood flow changes with common carotid compression (Makinaga), 637

modulation of middle cerebral artery flow velocity waveforms by breathing movements in the normal term fetus (Burghouwt), 821

new implanted Doppler sensors for the assessment of the main fetal hemodynamics (Arbeille), 97

reproducibility of transcranial Dopplersonography: a validation study (Totaro), 173

Céspedes, I., see Ponnekanti, H.
Céspedes, I., Ophir, J. and Huang, Y.: on the feasibility of pulse-echo speed of sound estimation in small regions: simulation studies, 283
Céspedes, I. and Ophir, J.: correction of diffraction errors in attenuation estimation with dynamic beam translation, 213

Chase, J. D., see Wu, J.

Cheung, A. H. S., Jiranek, G. C., Haggitt, R. C., Ferguson, D. C., Silverstein, F. E. and Perkins, J. D.: use of ultrasound to detect intestinal wall ischemia in piglets, 843

Chiang, E. H., see Alder, R. S.

Child, S. Z., Raeman, C. H., Walters, E. and Carstensen, E. L.: the sensitivity of *Drosophila* larvae to continuous-wave ultrasound, 725

Choi, M. J., see Coleman, A. J.

Circumferential fiber shortening
simultaneous cardio-cerebral ultrasonic measurement technique for assessing the interrelationship between cardiac and cerebral circulations in elderly subjects: a preliminary study (Matsumoto), 45

Cobbold, R. S. C., see Vera, N.

Coleman, A. J., Choi, M. J., Saunders, J. E. and Leighton, T. G.: acoustic emission and sonoluminescence due to cavitation at the beam focus of an electrohydraulic shock wave lithotripter, 267

Coleman, D. J., see Lizzi, F. L.

Collagen
correlations of liver echo intensity with cytology and chemical measurements of fat, water and protein content in live burbots (*Lota lota*) (Bondestam), 75

dependence of ultrasonic attenuation of liver on pathologic fat and fibrosis: examination with experimental fatty liver and liver fibrosis models (Suzuki), 657

Color flow Doppler
a method for computer simulation of ultrasound Doppler color flow images—I. Theory and numerical method (Kerr), 861

a method for computer simulation of ultrasound Doppler color flow images—II. Simulation results (Kerr), 873

a velocity evaluation phantom for colour and pulsed Doppler instruments (Rickey), 479

color Doppler characteristics in normal lower extremity arteries (Hatsukami), 167

colour Doppler velocity imaging of the myocardium (McDicken), 651

comparison of flow disturbances in small carotid atheroma using a multi-gate pulsed Doppler system and Doppler color flow imaging (Steinke), 11

quantification of Doppler color flow images from a stenosed carotid artery model (Vattyam), 195

the assessment of benign uterine tumor vascularization by transvaginal color Doppler (Kurjak), 645

visualization of complex flow fields, with application to the interpretation of colour flow Doppler images (Vera), 1

Color vector display
vector Doppler: accurate measurement of blood velocity in two dimensions (Overbeck), 19

visualization of complex flow fields, with application to the interpretation of colour flow Doppler images (Vera), 1

Colour imaging
colour Doppler velocity imaging of the myocardium (McDicken), 651

Complex flow
quantification of Doppler color flow images from a stenosed carotid artery model (Vattyam), 195

simulation of Doppler ultrasound signals for a laminar, pulsatile, nonuniform flow (Wendling), 179

vector Doppler: accurate measurement of blood velocity in two dimensions (Overbeck), 19

visualization of complex flow fields, with application to the interpretation of colour flow Doppler images (Vera), 1

Compliance
noninvasive measurement of diameter changes in the distal abdominal aorta in man (Länne), 451

Compression test
continuous and simultaneous ultrasound Doppler velocity of the internal carotid and vertebral arteries: preliminary observations of cerebral blood flow changes with common carotid compression (Makinaga), 637

Contrast agent
digital path-dependent recompensation of contrast-enhanced echocardiographic images (Mor-Avi), 831

Cooperberg, E.: ultrasound Doppler spectral analysis in the diagnosis of occlusive lesions of the carotid arteries, 421

Cow
sonic velocity and attenuation in wet compact cow femur for the frequency range 5 to 100 MHz (Lees), 303

Cow femur
sonic velocity and attenuation in wet compact cow femur for the frequency range 5 to 100 MHz (Lees), 303

Creutzig, A., see Ranke, C.

Cross-correlation
on the feasibility of pulse-echo speed of sound estimation in small regions: simulation studies (Céspedes), 283

pulse pressure assessment in the human fetal descending aorta (Struijk), 39

Crystal ball
1975–2000: a quarter century of ultrasound technology (Beach), 377

Cytotoxicity
ultrasound-enhanced effects of adriamycin against murine tumors (Saad), 715

D

Dahl, P., see Länne, T.

David, D., see Mor-Avi, V.

Debye effect
ultrasonic vibrational potentials in gels and preparations of biological tissue (Rosenfeld), 607

Decorrelation distance
on the feasibility of pulse-echo speed of sound estimation in small regions: simulation studies (Céspedes), 283

Dedrick, D. K., see Alder, R. S.

Delius, M., see Gambihler, S.

Diffraction correction
correction of diffraction errors in attenuation estimation with dynamic beam translation (Céspedes), 213

Dog
a comparison of theoretical and experimental ultrasound field distributions in canine muscle tissue *in vivo* (Moros), 81

cerebral blood flow velocity: the influence of myocardial contractility on the velocity waveform of brain supplying arteries (Van Bel), 441

identifying acoustic scattering sources in normal renal parenchyma *in vivo* by varying arterial and ureteral pressures (Insana), 587

Doida, Y., Brayman, A. A. and Miller, M. W.: modest enhancement of ultrasound-induced mutations in V79 cells *in vitro*, 465

Doida, Y., see Brayman, A. A.

Doppler
a method for computer simulation of ultrasound Doppler color flow images—I. Theory and numerical method (Kerr), 861

a method for computer simulation of ultrasound Doppler color flow images—II. Simulation results (Kerr), 873

a velocity evaluation phantom for colour and pulsed Doppler instruments (Rickey), 479

color Doppler characteristics in normal lower extremity arteries (Hatsukami), 167

colour Doppler velocity imaging of the myocardium (McDicken), 651

comparison of flow disturbances in small carotid atheroma using a multi-gate pulsed Doppler system and Doppler color flow imaging (Steinke), 11

computed estimates of maximum temperature elevations in fetal tissues during transabdominal pulsed Doppler examinations (Bly), 389

continuous and simultaneous ultrasound Doppler velocity of the internal carotid and vertebral arteries: preliminary observations of cerebral blood flow changes with common carotid compression (Makinaga), 637

ductus venosus blood flow velocity waveforms in the human fetus—a Doppler study (Huisman), 33

duplex scanning of the peripheral arteries: correlation of the peak velocity ratio with angiographic diameter reduction (Ranke), 433

factors determining aortic and umbilical blood flow pulsatility in fetal sheep (Adamson), 255

how useful are acceleration- and deceleration-based Doppler indices? A trial on patients with percutaneous transluminal angioplasty (Windeck), 525

modulation of middle cerebral artery flow velocity waveforms by breathing movements in the normal term fetus (Burghouwt), 821

new implanted Doppler sensors for the assessment of the main fetal hemodynamics (Arbeille), 97

pulse pressure assessment in the human fetal descending aorta (Struijk), 39

quantification of Doppler color flow images from a stenosed carotid artery model (Vattyam), 195

reproducibility of fetal cardiac flow velocity waveforms at atrioventricular level (van der Mooren), 827

reproducibility of transcranial Dopplersonography: a validation study (Totaro), 173

simulation of Doppler ultrasound signals for a laminar, pulsatile, nonuniform flow (Wendling), 179

simultaneous cardio-cerebral ultrasonic measurement technique for assessing the interrelationship between cardiac and cerebral circulations in elderly subjects: a preliminary study (Matsumoto), 45

temperature rise in a tissue-mimicking material generated by unfocused and focused ultrasonic transducers (Wu), 495

the assessment of benign uterine tumor vascularization by transvaginal color Doppler (Kurjak), 645

the early development of neurosonology: I. Echoencephalography in adults (White), 115

the early development of neurosonology: III. Pulsatile echoencephalography and Doppler techniques (White), 323

ultrasound Doppler spectral analysis in the diagnosis of occlusive lesions of the carotid arteries (Cooperberg), 421

vector Doppler: accurate measurement of blood velocity in two dimensions (Overbeck), 19

visualization of complex flow fields, with application to the interpretation of colour flow Doppler images (Vera), 1

Doppler indices

factors determining aortic and umbilical blood flow pulsatility in fetal sheep (Adamson), 255

how useful are acceleration- and deceleration-based Doppler indices? A trial on patients with percutaneous transluminal angioplasty (Windeck), 525

modelling the feto-placental circulation: 1. A distributed network predicting umbilical haemodynamics throughout pregnancy (Guiot), 535

modelling the feto-placental circulation: 2. A continuous approach to explain normal and abnormal flow velocity waveforms in the umbilical arteries (Todros), 545

new implanted Doppler sensors for the assessment of the main fetal hemodynamics (Arbeille), 97

Dosimetry

fetal exposure from endovaginal ultrasound examinations in the first trimester (Hussain), 675

human *in situ* dosimetry: differential insertion loss during passage through abdominal wall and myometrium (Siddiqi), 681

Driller, J., see Lizzi, F. L.

Drosophila

the sensitivity of *Drosophila* larvae to continuous-wave ultrasound (Child), 725

Dual energy CT
in vitro classification of gallstones by quantitative echography (Goedegebure), 553

Ductus venosus
ductus venosus blood flow velocity waveforms in the human fetus—a Doppler study (Huisman), 33

Duplex
duplex scanning of the peripheral arteries: correlation of the peak velocity ratio with angiographic diameter reduction (Ranke), 433

Dynamic beam translation
correction of diffraction errors in attenuation estimation with dynamic beam translation (Céspedes), 213

E

ECG
differentiation of normal and ischemic right ventricular myocardium with quantitative two-dimensional integrated backscatter imaging (Waggoner), 249

Echo intensity
correlations of liver echo intensity with cytology and chemical measurements of fat, water and protein content in live burbots (*Lota lota*) (Bondestam), 75

Echocardiography
differentiation of normal and ischemic right ventricular myocardium with quantitative two-dimensional integrated backscatter imaging (Waggoner), 249

simultaneous cardio-cerebral ultrasonic measurement technique for assessing the interrelationship between cardiac and cerebral circulations in elderly subjects: a preliminary study (Matsumoto), 45

the effect of heparin versus citrate on blood echogenicity *in vitro:* the role of platelet and platelet-neutrophil aggregates (Mahony), 851

Echoencephalography
the early development of neurosonology: I. Echoencephalography in adults (White), 115

the early development of neurosonology: II. Fetal and neonatal echoencephalography (White), 227

the early development of neurosonology: III. Pulsatile echoencephalography and Doppler techniques (White), 323

Echogenicity
red cell aggregation and the echogenicity of whole blood (Mahony), 579

the effect of heparin versus citrate on blood echogenicity *in vitro:* the role of platelet and platelet-neutrophil aggregates (Mahony), 851

Edmonds, P. D., see Prohaska, S. S.

Elastic modulus
noninvasive measurement of diameter changes in the distal abdominal aorta in man (Länne), 451

Elasticity
axial stress distributions between coaxial compressors in elastography: an analytical model (Ponnekanti), 667

Elastography
axial stress distributions between coaxial compressors in elastography: an analytical model (Ponnekanti), 667

Els, T., see Steinke, W.

Erythrocytes
apparent contribution of respiratory gas exchange to the *in vitro* "cell density effect" in ultrasonic cell lysis (Brayman), 701

red cell aggregation and the echogenicity of whole blood (Mahony), 579

ESWL
acoustic emission and sonoluminescence due to cavitation at the beam focus of an electrohydraulic shock wave lithotripter (Coleman), 267

an attempt to reconstruct the lithotripter shock wave pulse in kidney: possible temperature effects (Filipczyński), 569

influence of dissolved and free gases on iodine release and cell killing by shock waves *in vitro* (Gambihler), 617

in vitro investigations on cellular damage induced by high energy shock waves (Steinbach), 691

Ethier, C. R., see Vera, N.

Etienne, J., see Filipczyński, L.

Exposure
fetal exposure from endovaginal ultrasound examinations in the first trimester (Hussain), 675

human *in situ* dosimetry: differential insertion loss during passage through abdominal wall and myometrium (Siddiqi), 681

F

F number
correction of diffraction errors in attenuation estimation with dynamic beam translation (Céspedes), 213

Fat
correlations of liver echo intensity with cytology and chemical measurements of fat, water and protein content in live burbots (*Lota lota*) (Bondestam), 75

dependence of ultrasonic attenuation of liver on pathologic fat and fibrosis: examination with experimental fatty liver and liver fibrosis models (Suzuki), 657

Fay, B., Lewin, P. A., Ludwig, G., Sessler, G. M. and Yang, G.: the influence of spatial polarization distribution on spot poled PVDF membrane hydrophone performance, 625

Fein, M., Zuna, I. and Lorenz, W. J.: new method of estimating the ultrasonic beam ratio parameter for characterizing sound propagation in tissue, 881

Feleppa, E. J., see Loiacono, L. A.

Femur
sonic velocity and attenuation in wet compact cow femur for the frequency range 5 to 100 MHz (Lees), 303

Fenster, A., see Rickey, D. W.

Ferguson, D. C., see Cheung, A. H. S.

Ferguson, J., see Mahony, C.

Fetal blood flow
ductus venosus blood flow velocity waveforms in the human fetus—a Doppler study (Huisman), 33

pulse pressure assessment in the human fetal descending aorta (Struijk), 39

Fetal breathing
modulation of middle cerebral artery flow velocity waveforms by breathing movements in the normal term fetus (Burghouwt), 821

Fetal circulation
modelling the feto-placental circulation: 1. A distributed network predicting umbilical haemodynamics throughout pregnancy (Guiot), 535

modelling the feto-placental circulation: 2. A continuous approach to explain normal and abnormal flow velocity waveforms in the umbilical arteries (Todros), 545

modulation of middle cerebral artery flow velocity waveforms by breathing movements in the normal term fetus (Burghouwt), 821

new implanted Doppler sensors for the assessment of the main fetal hemodynamics (Arbeille), 97

pulse pressure assessment in the human fetal descending aorta (Struijk), 39

reproducibility of fetal cardiac flow velocity waveforms at atrioventricular level (van der Mooren), 827

Fetal heating
computed estimates of maximum temperature elevations in fetal tissues during transabdominal pulsed Doppler examinations (Bly), 389

Fetus
computed estimates of maximum temperature elevations in fetal tissues during transabdominal pulsed Doppler examinations (Bly), 389

ductus venous blood flow velocity waveforms in the human fetus—a Doppler study (Huisman), 33

fetal exposure from endovaginal ultrasound examinations in the first trimester (Hussain), 675

modelling the feto-placental circulation: 1. A distributed network predicting umbilical haemodynamics throughout pregnancy (Guiot), 535

modelling the feto-placental circulation: 2. A continuous approach to explain normal and abnormal flow velocity waveforms in the umbilical arteries (Todros), 545

modulation of middle cerebral artery flow velocity waveforms by breathing movements in the normal term fetus (Burghouwt), 821

new implanted Doppler sensors for the assessment of the main fetal hemodynamics (Arbeille), 97

pulse pressure assessment in the human fetal descending aorta (Struijk), 39

the early development of neurosonology: II. Fetal and neonatal echoencephalography (White), 227

FFT

simulation of Doppler ultrasound signals for a laminar, pulsatile, nonuniform flow (Wendling), 179

Fibrin mesh

cellularity and fibrin mesh properties as a basis for ultrasonic tissue characterization of blood clots and thrombi (Loiacono), 399

Fibroids

the assessment of benign uterine tumor vascularization by transvaginal color Doppler (Kurjak), 645

Fibrosis

dependence of ultrasonic attenuation of liver on pathologic fat and fibrosis: examination with experimental fatty liver and liver fibrosis models (Suzuki), 657

Filipczyński, L., Etienne, J. and Piechocki, M.: an attempt to reconstruct the lithotripter shock wave pulse in kidney: possible temperature effects, 569

Fischer, P. L. C., see Mahony, C.

Fish

correlations of liver echo intensity with cytology and chemical measurements of fat, water and protein content in live burbots (*Lota lota*) (Bondestam), 75

Flow

comparison of flow disturbances in small carotid atheroma using a multi-gate pulsed Doppler system and Doppler color flow imaging (Steinke), 11

how useful are acceleration- and deceleration-based Doppler indices? A trial on patients with percutaneous transluminal angioplasty (Windeck), 525

modelling the feto-placental circulation: 1. A distributed network predicting umbilical haemodynamics throughout pregnancy (Guiot), 535

modelling the feto-placental circulation: 2. A continuous approach to explain normal and abnormal flow velocity waveforms in the umbilical arteries (Todros), 545

modulation of middle cerebral artery flow velocity waveforms by breathing movements in the normal term fetus (Burghouwt), 821

new implanted Doppler sensors for the assessment of the main fetal hemodynamics (Arbeille), 97

quantification of Doppler color flow images from a stenosed carotid artery model (Vattyam), 195

simulation of Doppler ultrasound signals for a laminar, pulsatile, nonuniform flow (Wendling), 179

reproducibility of fetal cardiac flow velocity waveforms at atrioventricular level (van der Mooren), 827

the assessment of benign uterine tumor vascularization by transvaginal color Doppler (Kurjak), 645

visualization of complex flow fields, with application to the interpretation of colour flow Doppler images (Vera), 1

Flow phantom

quantification of Doppler color flow images from a stenosed carotid artery model (Vattyam), 195

simulation of Doppler ultrasound signals for a laminar, pulsatile, nonuniform flow (Wendling), 179

Flow profile

comparison of flow disturbances in small carotid atheroma using a multi-gate pulsed Doppler system and Doppler color flow imaging (Steinke), 11

ductus venous blood flow velocity waveforms in the human fetus—a Doppler study (Huisman), 33

quantification of Doppler color flow images from a stenosed carotid artery model (Vattyam), 195

visualization of complex flow fields, with application to the interpretation of colour flow Doppler images (Vera), 1

Flow velocity waveform

continuous and simultaneous ultrasound Doppler velocity of the internal carotid and vertebral arteries: preliminary observations of cerebral blood flow changes with common carotid compression (Makinaga), 637

ductus venosus blood flow velocity waveforms in the human fetus—a Doppler study (Huisman), 33

how useful are acceleration- and deceleration-based Doppler indices? A trial on patients with percutaneous transluminal angioplasty (Windeck), 525

modelling the feto-placental circulation: 1. A distributed network predicting umbilical haemodynamics throughout pregnancy (Guiot), 535

modelling the feto-placental circulation: 2. A continuous approach to explain normal and abnormal flow velocity waveforms in the umbilical arteries (Todros), 545

Fluid dynamics

comparison of flow disturbances in small carotid atheroma using a multi-gate pulsed Doppler system and Doppler color flow imaging (Steinke), 11

new implanted Doppler sensors for the assessment of the main fetal hemodynamics (Arbeille), 97

visualization of complex flow fields, with application to the interpretation of colour flow Doppler images (Vera), 1

Focused transducers

a comparison of theoretical and experimental ultrasound field distributions in canine muscle tissue *in vivo* (Moros), 81

an attempt to reconstruct the lithotripter shock wave pulse in kidney: possible temperature effects (Filipczyński), 569

correction of diffraction errors in attenuation estimation with dynamic beam translation (Céspedes), 213

temperature rise in a tissue-mimicking material generated by unfocused and focused ultrasonic transducers (Wu), 495

Focusing
a comparison of theoretical and experimental ultrasound field distributions in canine muscle tissue *in vivo* (Moros), 81

an attempt to reconstruct the lithotripter shock wave pulse in kidney: possible temperature effects (Filipczynski), 569

correction of diffraction errors in attenuation estimation with dynamic beam translation (Céspedes), 213

temperature rise generated by a focussed Gaussian beam in a two-layer medium (Wu), 293

temperature rise in a tissue-mimicking material generated by unfocused and focused ultrasonic transducers (Wu), 495

Fukuda, M.: message to subscribers, readers and contributors from the President of the World Federation for Ultrasound in Medicine and Biology, 523

Furukawa, T., see Makinaga, G.

Fusamoto, H., see Suzuki, K.

Future
1975–2000: a quarter century of ultrasound technology (Beach), 377

G

Gallstones
in vitro classification of gallstones by quantitative echography (Goedegebure), 553

Gambihler, S. and Delius, M.: influence of dissolved and free gases on iodine release and cell killing by shock waves *in vitro*, 617

Gas body activation
the sensitivity of *Drosophila* larvae to continuous-wave ultrasound (Child), 725

Gaussian beams
temperature rise generated by a focussed Gaussian beam in a two-layer medium (Wu), 293

temperature rise in a tissue-mimicking material generated by unfocused and focused ultrasonic transducers (Wu), 495

Giddens, D. P., see Wendling, F.

Goedegebure, A., van der Steen, A. F. W. and Thijssen, J. M.: *in vitro* classification of gallstones by quantitative echography, 553

Golub, R. M., see Loiacono, L. A.

Gordon, L. N., see McDicken, W. N.

Goriya, Y., see Matsumoto, M.

Grant, E. G., see Hussain, R.

Guiot, C., Piantà, P. G. and Todros, T.: modelling the feto-placental circulation: 1. A distributed network predicting umbilical haemodynamics throughout pregnancy, 535

Gustafsson, D., see Länne, T.

H

Haemodynamics
modelling the feto-placental circulation: 1. A distributed network predicting umbilical haemodynamics throughout pregnancy (Guiot), 535

modelling the feto-placental circulation: 2. A continuous approach to explain normal and abnormal flow velocity waveforms in the umbilical arteries (Todros), 545

new implanted Doppler sensors for the assessment of the main fetal hemodynamics (Arbeille), 97

Haggitt, R. C., see Cheung, A. H. S.

Hahn, G. M., see Saad, A. H.

Hall, T. J., see Insana, M. F.

Hatsukami, T. S., Primozich, J., Zierler, R. E. and Strandness, D. E., Jr.: color Doppler characteristics in normal lower extremity arteries, 167

Hayashi, N., see Suzuki, K.

Heating
an attempt to reconstruct the lithotripter shock wave pulse in kidney: possible temperature effects (Filipczyński), 569

computed estimates of maximum temperature elevations in fetal tissues during transabdominal pulsed Doppler examinations (Bly), 389

computer model of ultrasonic hyperthermia and ablation for ocular tumors using B-mode data (Lizzi), 59

effect of ultrasound on the neonatal rat brain (Margulies), 459

temperature rise generated by a focussed Gaussian beam in a two-layer medium (Wu), 293

temperature rise in a tissue-mimicking material generated by unfocused and focused ultrasonic transducers (Wu), 495

Hematocrit
red cell aggregation and the echogenicity of whole blood (Mahony), 579

Hennerici, M., see Steinke, W.

Heparin
the effect of heparin versus citrate on blood echogenicity *in vitro:* the role of platelet and platelet-neutrophil aggregates (Mahony), 851

High resolution
high-resolution real-time ultrasonic scanner (Berson), 471

Histomorphology
correlations of liver echo intensity with cytology and chemical measurements of fat, water and protein content in live burbots (*Lota lota*) (Bondestam), 75

identifying acoustic scattering sources in normal renal parenchyma *in vivo* by varying arterial and ureteral pressures (Insana), 587

History

1975–2000: a quarter century of ultrasound technology (Beach), 377

the early development of neurosonology: I. Echoencephalography in adults (White), 115

the early development of neurosonology: II. Fetal and neonatal echoencephalography (White), 227

the early development of neurosonology: III. Pulsatile echoencephalography and Doppler techniques (White), 323

Hofstädter, F., see Steinbach, P.

Holzapfel, T. P., see Wu, J.

Homeostasis

simultaneous cardio-cerebral ultrasonic measurement technique for assessing the interrelationship between cardiac and cerebral circulations in elderly subjects: a preliminary study (Matsumoto), 45

Hop, W. C. J., see van der Mooren, K.

Hop, W. C. J., see Struijk, P. C.

Huang, Y., see Céspedes, I.

Huisman, T. W. A., Stewart, P. A. and Wladimiroff, J. W.: ductus venosus blood flow velocity waveforms in the human fetus—a Doppler study, 33

Hunt, J. W., see Kerr, A. T.

Hussain, R., Kimme-Smith, C., Tessler, F. N., Perrella, R. R., Grant, E. G. and Sandstrom, K.: fetal exposure from endovaginal ultrasound examinations in the first trimester, 675

Hussey, R. G., see Bly, S. H. P.

Hydrophones

human *in situ* dosimetry: differential insertion loss during passage through abdominal wall and myometrium (Siddiqi), 681

the influence of spatial polarization distribution on spot poled PVDF membrane hydrophone performance (Fay), 625

Hynynen, K., see Moros, E. G.

Hyperthermia

a comparison of theoretical and experimental ultrasound field distributions in canine muscle tissue *in vivo* (Moros), 81

computer model of ultrasonic hyperthermia and ablation for ocular tumors using B-mode data (Lizzi), 59

temperature rise in a tissue-mimicking material generated by unfocused and focused ultrasonic transducers (Wu), 495

ultrasound-enhanced effects of adriamycin against murine tumors (Saad), 715

I

Image processing

adaptive time gain compensation for ultrasonic imaging (Pye), 205

new method of estimating the ultrasonic beam ratio parameter for characterizing sound propagation in tissue (Fein), 881

Image texture
new method of estimating the ultrasonic beam ratio parameter for characterizing sound propagation in tissue (Fein), 881

Imaging
adaptive time gain compensation for ultrasonic imaging (Pye), 205

architectural distortion of subcutaneous fascial layer in breast tumors: ultrasonographic evaluation (Nishimura), 815

colour Doppler velocity imaging of the myocardium (McDicken), 651

high-resolution real-time ultrasonic scanner (Berson), 471

new method of estimating the ultrasonic beam ratio parameter for characterizing sound propagation in tissue (Fein), 881

use of ultrasound to detect intestinal wall ischemia in piglets (Cheung), 843

Imai, Y., see Suzuki, K.

Implanted Doppler
new implanted Doppler sensors for the assessment of the main fetal hemodynamics (Arbeille), 97

Insana, M. F., Wood, J. G. and Hall, T. J.: identifying acoustic scattering sources in normal renal parenchyma *in vivo* by varying arterial and ureteral pressures, 587

Intestinal wall
use of ultrasound to detect intestinal wall ischemia in piglets (Cheung), 843

in vitro *irradiation*
apparent contribution of respiratory gas exchange to the *in vitro* "cell density effect" in ultrasonic cell lysis (Brayman), 701

bubble cycling and standing waves in ultrasonic cell lysis (Brayman), 411

computer model of ultrasonic hyperthermia and ablation for ocular tumors using B-mode data (Lizzi), 59

conservation of bactericidal activity in ultrasound-exposed murine peritoneal phagocytic cells (Prohaska), 601

influence of dissolved and free gases on iodine release and cell killing by shock waves *in vitro* (Gambihler), 617

in vitro investigations on cellular damage induced by high energy shock waves (Steinbach), 691

modest enhancement of ultrasound-induced mutations in V79 cells *in vitro* (Doida), 465

ultrasonic vibrational potentials in gels and preparations of biological tissue (Rosenfeld), 607

in vivo *irradiation*
effect of ultrasound on the neonatal rat brain (Margulies), 459

the sensitivity of *Drosophila* larvae to continuous-wave ultrasound (Child), 725

ultrasound-enhanced effects of adriamycin against murine tumors (Saad), 715

Iodine yield
influence of dissolved and free gases on iodine release and cell killing by shock waves *in vitro* (Gambihler), 617

Irradiation
apparent contribution of respiratory gas exchange to the *in vitro* "cell density effect" in ultrasonic cell lysis (Brayman), 701

bubble cycling and standing waves in ultrasonic cell lysis (Brayman), 411

computer model of ultrasonic hyperthermia and ablation for ocular tumors using B-mode data (Lizzi), 59

conservation of bactericidal activity in ultrasound-exposed murine peritoneal phagocytic cells (Prohaska), 601

effect of ultrasound on the neonatal rat brain (Margulies), 459

influence of dissolved and free gases on iodine release and cell killing by shock waves *in vitro* (Gambihler), 617

in vitro investigations on cellular damage induced by high energy shock waves (Steinbach), 691

modest enhancement of ultrasound-induced mutations in V79 cells *in vitro* (Doida), 465

the sensitivity of *Drosophila* larvae to continuous-wave ultrasound (Child), 725

ultrasonic vibrational potentials in gels and preparations of biological tissue (Rosenfeld), 607

ultrasound-enhanced effects of adriamycin against murine tumors (Saad), 715

Ischemia
differentiation of normal and ischemic right ventricular myocardium with quantitative two-dimensional integrated backscatter imaging (Waggoner), 249

use of ultrasound to detect intestinal wall ischemia in piglets (Cheung), 843

Isotherm
computer model of ultrasonic hyperthermia and ablation for ocular tumors using B-mode data (Lizzi), 59

IVC
ductus venosus blood flow velocity waveforms in the human fetus—a Doppler study (Huisman), 33

J

Jaeger, K. A., see Windeck, P.

Jiranek, G. C., see Cheung, A. H. S.

Johnston, K. W., see Vera, N.

Jones, S. A., see Wendling, F.

Justin, J., see Loiacono, L. A.

K

Kalisz, A., see Lizzi, F. L.

Kamada, T., see Suzuki, K.

Kaneko, Z., see Makinaga, G.

Kasahara, A., see Suzuki, K.

Kashihara, S., see Nishimura, S.

Kerr, A. T. and Hunt, J. W.: a method for computer simulation of ultrasound Doppler color flow images—I. Theory and numerical method, 861

Kerr, A. T. and Hunt, J. W.: a method for computer simulation of ultrasound Doppler color flow images—II. Simulation results, 873

Keselbrener, L., see Mor-Avi, V.

Kidney

an attempt to reconstruct the lithotripter shock wave pulse in kidney: possible temperature effects (Filipczyński), 569

identifying acoustic scattering sources in normal renal parenchyma *in vivo* by varying arterial and ureteral pressures (Insana), 587

Kimitsuki, H., see Loiacono, L. A.

Kimme-Smith, C., see Hussain, R.

Klopholz, D. Z., see Lees, S.

Kodama, I., see Loiacono, L. A.

Koizumi, S., see Nishimura, S.

Kondo, H., see Makinaga, G.

Kono, M., see Suzuki, K.

Kupesic-Urek, S., see Kurjak, A.

Kurjak, A., Kupesic-Urek, S. and Miric, D.: the assessment of benign uterine tumor vascularization by transvaginal color Doppler, 645

L

L1210

influence of dissolved and free gases on iodine release and cell killing by shock waves *in vitro* (Gambihler), 617

Labs, K.-H., see Windeck, P.

Laing, T. J., see Alder, R. S.

Langille, B. L., see Adamson, S. L.

Länne, T., Stale, H., Bengtsson, H., Gustafsson, D., Bergqvist, D., Sonesson, B., Lecerof, H. and Dahl, P.: noninvasive measurement of diameter changes in the distal abdominal aorta in man, 451

Lecerof, H., see Länne, T.

Lees, S. and Klopholz, D. Z.: sonic velocity and attenuation in wet compact cow femur for the frequency range 5 to 100 MHz, 303

Leighton, T. G., see Coleman, A. J.

Lewin, P. A., see Fay, B.

Light, L. H.: measures of cardiac output, 309L

Lithotripsy
acoustic emission and sonoluminescence due to cavitation at the beam focus of an electrohydraulic shock wave lithotripter (Coleman), 267

an attempt to reconstruct the lithotripter shock wave pulse in kidney: possible temperature effects (Filipczynski), 569

influence of dissolved and free gases on iodine release and cell killing by shock waves *in vitro* (Gambihler), 617

in vitro investigations on cellular damage induced by high energy shock waves (Steinbach), 691

Liver
correlations of liver echo intensity with cytology and chemical measurements of fat, water and protein content in live burbots (*Lota lota*) (Bondestam), 75

dependence of ultrasonic attenuation of liver on pathologic fat and fibrosis: examination with experimental fatty liver and liver fibrosis models (Suzuki), 657

Lizzi, F. L., Driller, J., Lunzer, B., Kalisz, A. and Coleman, D. J.: computer model of ultrasonic hyperthermia and ablation for ocular tumors using B-mode data, 59

Locatelli, A., see Arbeille, Ph.

Loiacono, L. A., Sigel, B., Feleppa, E. J., Swami, V. K., Parsons, R. E., Justin, J., Yaremko, M. M., Rorke, M., Kodama, I., Golub, R. M. and Kimitsuki, H.: cellularity and fibrin mesh properties as a basis for ultrasonic tissue characterization of blood clots and thrombi, 399

Lorenz, W. J., see Fein, M.

Lota lota
correlations of liver echo intensity with cytology and chemical measurements of fat, water and protein content in live burbots (*Lota lota*) (Bondestam), 75

Lower extremity arteries
color Doppler characteristics in normal lower extremity arteries (Hatsukami), 167

Ludwig, G., see Fay, B.

Lunzer, B., see Lizzi, F. L.

M

Mabee, P. R., see Bly, S. H. P.

Macrophages
conservation of bactericidal activity in ultrasound-exposed murine peritoneal phagocytic cells (Prohaska), 601

Magee, T. R. and Davies, A. H.: protection of bilateral transcranial Doppler transducers during interoperative monitoring, 515L

Mahony, C., Ferguson, J. and Fischer, P. L. C.: red cell aggregation and the echogenicity of whole blood, 579

Mahony, C. and Ferguson, J.: the effect of heparin versus citrate on blood echogenicity *in vitro:* the role of platelet and platelet-neutrophil aggregates, 851

Makinaga, G., Kondo, H., Ochi, N., Akashi, K., Furukawa, T., Matsumura, K., Tanaka, S., Nishimura, T. and Kaneko, Z.: continuous and simultaneous ultrasound Doppler velocity of the internal carotid and vertebral arteries: preliminary observations of cerebral blood flow changes with common carotid compression, 637

Margulies, N., Abraham, V., Way, J. S. and Ziskin, M. C.: effect of ultrasound on the neonatal rat brain, 459

Marini, C., see Totaro, R.

Matsumoto, M., see Matsumoto, M.

Matsumoto, M., Sekimoto, H., Goriya, Y., Matsumoto, M., Tsuchiya, H., Takasaki, M. and Takizawa, S.: simultaneous cardio-cerebral ultrasonic measurement technique for assessing the interrelationship between cardiac and cerebral circulations in elderly subjects: a preliminary study, 45

Matsumura, K., see Makinaga, G.

Matsusue, S., see Nishimura, S.

Maulik, D., see Arbeille, Ph.

McDicken, W. N., see Pye, S. D.

McDicken, W. N., Sutherland, G. R., Moran, C. M. and Gordon, L. N.: colour Doppler velocity imaging of the myocardium, 651

Meyer, C. R., see Alder, R. S.

Meyer, R. A., see Siddiqi, T. A.

Microscopic anatomy

identifying acoustic scattering sources in normal renal parenchyma *in vivo* by varying arterial and ureteral pressures (Insana), 587

Middle cerebral artery

modulation of middle cerebral artery flow velocity waveforms by breathing movements in the normal term fetus (Burghouwt), 821

reproducibility of transcranial Dopplersonography: a validation study (Totaro), 173

Midline

the early development of neurosonology: I. Echoencephalography in adults (White), 115

Miller, J. G., see Waggoner, A. D.

Miller, M. W., see Brayman, A. A.

Miller, M. W., see Brayman, A. A.

Miller, M. W., see Doida, Y.

Miodovnik, M., see Siddiqi, T. A.

Miric, D., see Kurjak, A.

Model

a comparison of theoretical and experimental ultrasound field distributions in canine muscle tissue *in vivo* (Moros), 81

a method for computer simulation of ultrasound Doppler color flow images—I. Theory and numerical method (Kerr), 861

a method for computer simulation of ultrasound Doppler color flow images—II. Simulation results (Kerr), 873

a velocity evaluation phantom for colour and pulsed Doppler instruments (Rickey), 479

axial stress distributions between coaxial compressors in elastography: an analytical model (Ponnekanti), 667

cerebral blood flow velocity: the influence of myocardial contractility on the velocity waveform of brain supplying arteries (Van Bel), 441

computed estimates of maximum temperature elevations in fetal tissues during transabdominal pulsed Doppler examinations (Bly), 389

computer model of ultrasonic hyperthermia and ablation for ocular tumors using B-mode data (Lizzi), 59

correction of diffraction errors in attenuation estimation with dynamic beam translation (Céspedes), 213

dependence of ultrasonic attenuation of liver on pathologic fat and fibrosis: examination with experimental fatty liver and liver fibrosis models (Suzuki), 657

digital path-dependent recompensation of contrast-enhanced echocardiographic images (Mor-Avi), 831

modelling the feto-placental circulation: 1. A distributed network predicting umbilical haemodynamics throughout pregnancy (Guiot), 535

modelling the feto-placental circulation: 2. A continuous approach to explain normal and abnormal flow velocity waveforms in the umbilical arteries (Todros), 545

new implanted Doppler sensors for the assessment of the main fetal hemodynamics (Arbeille), 97

on the feasibility of pulse-echo speed of sound estimation in small regions: simulation studies (Céspedes), 283

quantification of Doppler color flow images from a stenosed carotid artery model (Vattyam), 195

simulation of Doppler ultrasound signals for a laminar, pulsatile, nonuniform flow (Wendling), 179

sonic velocity and attenuation in wet compact cow femur for the frequency range 5 to 100 MHz (Lees), 303

temperature rise generated by a focussed Gaussian beam in a two-layer medium (Wu), 293

temperature rise in a tissue-mimicking material generated by unfocused and focused ultrasonic transducers (Wu), 495

the influence of spatial polarization distribution on spot poled PVDF membrane hydrophone performance (Fay), 625

visualization of complex flow fields, with application to the interpretation of colour flow Doppler images (Vera), 1

van der Mooren, K., Wladimiroff, J. W. and Hop, W. C. J.: reproducibility of fetal cardiac flow velocity waveforms at atrioventricular level, 827

Mor-Avi, V., Akselrod, S., David, D. and Keselbrener, L.: digital path-dependent recompensation of contrast-enhanced echocardiographic images, 831

Moran, C. M., see McDicken, W. N.

Moros, E. G. and Hynynen, K.: a comparison of theoretical and experimental ultrasound field distributions in canine muscle tissue *in vivo,* 81

Mucosa
use of ultrasound to detect intestinal wall ischemia in piglets (Cheung), 843

Müller, H. R.: a probe holder for bilateral transcranial Doppler sonography, 105L

Murine peritoneal macrophages
conservation of bactericidal activity in ultrasound-exposed murine peritoneal phagocytic cells (Prohaska), 601

Muscularis propria
use of ultrasound to detect intestinal wall ischemia in piglets (Cheung), 843

Mutation
modest enhancement of ultrasound-induced mutations in V79 cells *in vitro* (Doida), 465

Myocardium
cerebral blood flow velocity: the influence of myocardial contractility on the velocity waveform of brain supplying arteries (Van Bel), 441

colour Doppler velocity imaging of the myocardium (McDicken), 651

differentiation of normal and ischemic right ventricular myocardium with quantitative two-dimensional integrated backscatter imaging (Waggoner), 249

N

Neonatal rat brain
effect of ultrasound on the neonatal rat brain (Margulies), 459

Neurosonology
the early development of neurosonology: I. Echoencephalography in adults (White), 115

the early development of neurosonology: II. Fetal and neonatal echoencephalography (White), 227

the early development of neurosonology: III. Pulsatile echoencephalography and Doppler techniques (White), 323

Nicolai, H., see Steinbach, P.

Nishimura, S., Matsusue, S., Koizumi, S. and Kashihara, S.: architectural distortion of subcutaneous fascial layer in breast tumors: ultrasonographic evaluation, 815

Nishimura, T., see Makinaga, G.

Nonaxial flow
vector Doppler: accurate measurement of blood velocity in two dimensions (Overbeck), 19

Noncavitational bioeffects
ultrasonic vibrational potentials in gels and preparations of biological tissue (Rosenfeld), 607

Nonthermal bioeffects
ultrasonic vibrational potentials in gels and preparations of biological tissue (Rosenfeld), 607

Numerical models
a comparison of theoretical and experimental ultrasound field distributions in canine muscle tissue *in vivo* (Moros), 81

correction of diffraction errors in attenuation estimation with dynamic beam translation (Céspedes), 213

on the feasibility of pulse-echo speed of sound estimation in small regions: simulation studies (Céspedes), 283

simulation of Doppler ultrasound signals for a laminar, pulsatile, nonuniform flow (Wendling), 179

Nyborg, W. L., see Wu, J.

O

O'Brien, W. D., Jr., see Siddiqi, T. A.

Ochi, N., see Makinaga, G.

Ocular tumour
computer model of ultrasonic hyperthermia and ablation for ocular tumors using B-mode data (Lizzi), 59

Ophir, J., see Céspedes, I.
Ophir, J., see Céspedes, I.
Ophir, J., see Ponnekanti, H.

Osteoarthritis
quantitative assessment of cartilage surface roughness in osteoarthritis using high frequency ultrasound (Alder), 51

Overbeck, J. R., Beach, K. W. and Strandness, D. E., Jr.: vector Doppler: accurate measurement of blood velocity in two dimensions, 19

P

Parsons, R. E., see Loiacono, L. A.

Patat, F., see Berson, M.

Peak velocity ratio
duplex scanning of the peripheral arteries: correlation of the peak velocity ratio with angiographic diameter reduction (Ranke), 433

Pérez, J. E., see Waggoner, A. D.

Peripheral arteries
color Doppler characteristics in normal lower extremity arteries (Hatsukami), 167

duplex scanning of the peripheral arteries: correlation of the peak velocity ratio with angiographic diameter reduction (Ranke), 433

Perkins, J. D., see Cheung, A. H. S.

Perrella, R. R., see Hussain, R.

Phantom
a method for computer simulation of ultrasound Doppler color flow images—II. Simulation results (Kerr), 873

temperature rise in a tissue-mimicking material generated by unfocused and focused ultrasonic transducers (Wu), 495

Phase aberration
correction of diffraction errors in attenuation estimation with dynamic beam translation (Céspedes), 213

PI
how useful are acceleration- and deceleration-based Doppler indices? A trial on patients with percutaneous transluminal angioplasty (Windeck), 525

modelling the feto-placental circulation: 1. A distributed network predicting umbilical haemodynamics throughout pregnancy (Guiot), 535

modelling the feto-placental circulation: 2. A continuous approach to explain normal and abnormal flow velocity waveforms in the umbilical arteries (Todros), 545

Piantà, P. G., see Guiot, C.

Piechocki, M., see Filipczyński, L.

Piglet
use of ultrasound to detect intestinal wall ischemia in piglets (Cheung), 843

Placental flow
modelling the feto-placental circulation: 1. A distributed network predicting umbilical haemodynamics throughout pregnancy (Guiot), 535

modelling the feto-placental circulation: 2. A continuous approach to explain normal and abnormal flow velocity waveforms in the umbilical arteries (Todros), 545

Plaque
comparison of flow disturbances in small carotid atheroma using a multi-gate pulsed Doppler system and Doppler color flow imaging (Steinke), 11

Platelets
cellularity and fibrin mesh properties as a basis for ultrasonic tissue characterization of blood clots and thrombi (Loiacono), 399

the effect of heparin versus citrate on blood echogenicity *in vitro:* the role of platelet and platelet-neutrophil aggregates (Mahony), 851

Ponnekanti, H., Ophir, J. and Cespedes, I.: axial stress distributions between coaxial compressors in elastography: an analytical model, 667

Posterior cerebral artery
modulation of middle cerebral artery flow velocity waveforms by breathing movements in the normal term fetus (Burghouwt), 821

reproducibility of transcranial Dopplersonography: a validation study (Totaro), 173

Pourcelot, L., see Berson, M.

Prediction
1975–2000: a quarter century of ultrasound technology (Beach), 377

Prencipe, M., see Totaro, R.

Pressure waveforms
acoustic emission and sonoluminescence due to cavitation at the beam focus of an electrohydraulic shock wave lithotripter (Coleman), 267

an attempt to reconstruct the lithotripter shock wave pulse in kidney: possible temperature effects (Filipczyński), 569

the influence of spatial polarization distribution on spot poled PVDF membrane hydrophone performance (Fay), 625

Primozich, J., see Hatsukami, T. S.

Prohaska, S. S., Rimer, V. G., Tusé, D., Pryor, G. T. and Edmonds, P. D.: conservation of bactericidal activity in ultrasound-exposed murine peritoneal phagocytic cells, 601

Propagation
new method of estimating the ultrasonic beam ratio parameter for characterizing sound propagation in tissue (Fein), 881

Protein
correlations of liver echo intensity with cytology and chemical measurements of fat, water and protein content in live burbots (*Lota lota*) (Bondestam), 75

Pryor, G. T., see Prohaska, S. S.

PTA
how useful are acceleration- and deceleration-based Doppler indices? A trial on patients with percutaneous transluminal angioplasty (Windeck), 525

Pulse wave velocity
pulse pressure assessment in the human fetal descending aorta (Struijk), 39

PVDF
the influence of spatial polarization distribution on spot poled PVDF membrane hydrophone performance (Fay), 625

Pye, S. D., Wild, S. R. and McDicken, W. N.: adaptive time gain compensation for ultrasonic imaging, 205

Q

Quality assurance
a method for computer simulation of ultrasound Doppler color flow images—II. Simulation results (Kerr), 873

modest enhancement of ultrasound-induced mutations in V79 cells *in vitro* (Doida), 465

the influence of spatial polarization distribution on spot poled PVDF membrane hydrophone performance (Fay), 625

R

Rabbit
dependence of ultrasonic attenuation of liver on pathologic fat and fibrosis:

examination with experimental fatty liver and liver fibrosis models (Suzuki), 657

Raeman, C. H., see Child, S. Z.

Ranke, C., Creutzig, A. and Alexander, K.: duplex scanning of the peripheral arteries: correlation of the peak velocity ratio with angiographic diameter reduction, 433

Rankin, R., see Rickey, D. W.

Rats
effect of ultrasound on the neonatal rat brain (Margulies), 459

Real-time scanner
high-resolution real-time ultrasonic scanner (Berson), 471

Red cell aggregation
red cell aggregation and the echogenicity of whole blood (Mahony), 579

Renal stones
an attempt to reconstruct the lithotripter shock wave pulse in kidney: possible temperature effects (Filipczyński), 569

Reproducibility
reproducibility of fetal cardiac flow velocity waveforms at atrioventricular level (van der Mooren), 827

reproducibility of transcranial Dopplersonography: a validation study (Totaro), 173

Resolution
high-resolution real-time ultrasonic scanner (Berson), 471

Respirometry
apparent contribution of respiratory gas exchange to the *in vitro* "cell density effect" in ultrasonic cell lysis (Brayman), 701

Reviews, book
Diagnostic ultrasound: Reimack, Wilson and Charboneau (Greenbaum), 891

Endosonography: Fornage (Fleischer), 219

RF B-mode
in vitro classification of gallstones by quantitative echography (Goedegebure), 553

Rickey, D. W., Rankin, R. and Fenster, A.: a velocity evaluation phantom for colour and pulsed Doppler instruments, 479

Right ventricle
differentiation of normal and ischemic right ventricular myocardium with quantitative two-dimensional integrated backscatter imaging (Waggoner), 249

Rimer, V. G., see Prohaska, S. S.

Rittgers, S. E., see Vattyam, H. M.

Rorke, M., see Loiacono, L. A.

Rosenfeld, E. H.: ultrasonic vibrational potentials in gels and preparations of biological tissue, 607

Rössler, W., see Steinbach, P.

Rubin, J. M., see Alder, R. S.

S

Saad, A. H. and Hahn, G. M.: ultrasound-enhanced effects of adriamycin against murine tumors, 715

Safety

computed estimates of maximum temperature elevations in fetal tissues during transabdominal pulsed Doppler examinations (Bly), 389

conservation of bactericidal activity in ultrasound-exposed murine peritoneal phagocytic cells (Prohaska), 601

fetal exposure from endovaginal ultrasound examinations in the first trimester (Hussain), 675

human *in situ* dosimetry: differential insertion loss during passage through abdominal wall and myometrium (Siddiqi), 681

temperature rise generated by a focussed Gaussian beam in a two-layer medium (Wu), 293

temperature rise in a tissue-mimicking material generated by unfocused and focused ultrasonic transducers (Wu), 495

ultrasonic vibrational potentials in gels and preparations of biological tissue (Rosenfeld), 607

see also UMB 18 (9)

Sandstrom, K., see Hussain, R.

Sasaki, Y., see Suzuki, K.

Saunders, J. E., see Coleman, A. J.

Scattering

a comparison of theoretical and experimental ultrasound field distributions in canine muscle tissue *in vivo* (Moros), 81

a method for computer simulation of ultrasound Doppler color flow images—I. Theory and numerical method (Kerr), 861

a velocity evaluation phantom for colour and pulsed Doppler instruments (Rickey), 479

digital path-dependent recompensation of contrast-enhanced echocardiographic images (Mor-Avi), 831

the effect of herparin versus citrate on blood echogenicity *in vitro:* the role of platelet and platelet-neutrophil aggregates (Mahony), 851

Sekimoto, H., see Matsumoto, M.

Serosa

use of ultrasound to detect intestinal wall ischemia in piglets (Cheung), 843

Sessler, G. M., see Fay, B.

Shock waves
acoustic emission and sonoluminescence due to cavitation at the beam focus of an electrohydraulic shock wave lithotripter (Coleman), 267

influence of dissolved and free gases on iodine release and cell killing by shock waves *in vitro* (Gambihler), 617

in vitro investigations on cellular damage induced by high energy shock waves (Steinbach), 691

modest enhancement of ultrasound-induced mutations in V79 cells *in vitro* (Doida), 465

Shu, M. C. S., see Vattyam, H. M.

Siddiqi, T. A., O'Brien, W. D., Jr., Meyer, R. A., Sullivan, J. M. and Miodovnik, M.: human *in situ* dosimetry: differential insertion loss during passage through abdominal wall and myometrium, 681

Side lobes
a comparison of theoretical and experimental ultrasound field distributions in canine muscle tissue *in vivo* (Moros), 81

Sigel, B., see Loiacono, L. A.

Silverstein, F. E., see Cheung, A. H. S.

Simonazzi, E., see Struijk, P. C.

Simulation
simulation of Doppler ultrasound signals for a laminar, pulsatile, nonuniform flow (Wendling), 179

visualization of complex flow fields, with application to the interpretation of colour flow Doppler images (Vera), 1

Skin
high-resolution real-time ultrasonic scanner (Berson), 471

Skull
the early development of neurosonology: I. Echoencephalography in adults (White), 115

the early development of neurosonology: II. Fetal and neonatal echoencephalography (White), 227

the early development of neurosonology: III. Pulsatile echoencephalography and Doppler techniques (White), 323

Sobel, B. E., see Waggoner, A. D.

Sonesson, B., see Länne, T.

Sonoluminescence
acoustic emission and sonoluminescence due to cavitation at the beam focus of an electrohydraulic shock wave lithotripter (Coleman), 267

Sound speed
on the feasibility of pulse-echo speed of sound estimation in small regions: simulation studies (Céspedes), 283

Speckle
new method of estimating the ultrasonic beam ratio parameter for characterizing sound propagation in tissue (Fein), 881

Stale, H., see Länne, T.

Standing waves
bubble cycling and standing waves in ultrasonic cell lysis (Brayman), 411

Starritt, H. C. and Duck, F. A.: quantification of acoustic shock in routine exposure measurement, 513L

van der Steen, A. F. W., see Goedegebure, A.

Steendijk, P., see Van Bel, F.

Steinbach, P., Hofstädter, F., Nicolai, H., Rössler, W. and Wieland, W.: *in vitro* investigations on cellular damage induced by high energy shock waves, 691

Steinke, W., Els, T. and Hennerici, M.: comparison of flow disturbances in small carotid atheroma using a multi-gate pulsed Doppler system and Doppler color flow imaging, 11

Steinman, D. A., see Vera, N.

Stenosis
duplex scanning of the peripheral arteries: correlation of the peak velocity ratio with angiographic diameter reduction (Ranke), 433

quantification of Doppler color flow images from a stenosed carotid artery model (Vattyam), 195

Stewart, P. A., see Huisman, T. W. A.

Strain
axial stress distributions between coaxial compressors in elastography: an analytical model (Ponnekanti), 667

Strandness, D. E., Jr., see Hatsukami, T. S.
Strandness, D. E., Jr., see Overbeck, J. R.

Stress
axial stress distributions between coaxial compressors in elastography: an analytical model (Ponnekanti), 667

Struijk, P. C., Wladimiroff, J. W., Hop, W. C. J. and Simonazzi, E.: pulse pressure assessment in the human fetal descending aorta, 39

Subcutaneous fascial layer
architectural distortion of subcutaneous fascial layer in breast tumors: ultrasonographic evaluation (Nishimura), 815

Submucosa
use of ultrasound to detect intestinal wall ischemia in piglets (Cheung), 843

Sullivan, J. M., see Siddiqi, T. A.

Surface roughness
quantitative assessment of cartilage surface roughness in osteoarthritis using high frequency ultrasound (Alder), 51

Sutherland, G. R., see McDicken, W. N.

Suzuki, K., Hayashi, N., Sasaki, Y., Kono, M., Kasahara, A., Fusamoto, H., Imai, Y. and Kamada, T.: dependence of ultrasonic attenuation of liver on pathologic fat and fibrosis: examination with experimental fatty liver and liver fibrosis models, 657

Swami, V. K., see Loiacono, L. A.

Swept gain
adaptive time gain compensation for ultrasonic imaging (Pye), 205

digital path-dependent recompensation of contrast-enhanced echocardiographic images (Mor-Avi), 831

T

Takasaki, M., see Matsumoto, M.

Takizawa, S., see Matsumoto, M.

Tanaka, S., see Makinaga, G.

TCD
a probe holder for bilateral transcranial Doppler sonography (Muller), 105L

protection of bilateral transcranial Doppler transducers during interoperative monitoring (Magee), 515L

reproducibility of transcranial Dopplersonography: a validation study (Totaro), 173

Teitel, D. F., see Van Bel, F.

Tessler, F. N., see Hussain, R.

Therapeutic ultrasound
computer model of ultrasonic hyperthermia and ablation for ocular tumors using B-mode data (Lizzi), 59

in vitro investigations on cellular damage induced by high energy shock waves (Steinbach), 691

Thermal effects
an attempt to reconstruct the lithotripter shock wave pulse in kidney: possible temperature effects (Filipczyński), 569

computed estimates of maximum temperature elevations in fetal tissues during transabdominal pulsed Doppler examinations (Bly), 389

computer model of ultrasonic hyperthermia and ablation for ocular tumors using B-mode data (Lizzi), 59

effect of ultrasound on the neonatal rat brain (Margulies), 459

temperature rise generated by a focussed Gaussian beam in a two-layer medium (Wu), 293

temperature rise in a tissue-mimicking material generated by unfocused and focused ultrasonic transducers (Wu), 495

Thijssen, J. M., see Goedegebure, A.

Thrombus
cellularity and fibrin mesh properties as a basis for ultrasonic tissue characterization of blood clots and thrombi (Loiacono), 399

red cell aggregation and the echogenicity of whole blood (Mahony), 579

Time gain compensation
adaptive time gain compensation for ultrasonic imaging (Pye), 205

digital path-dependent recompensation of contrast-enhanced echocardiographic images (Mor-Avi), 831

Tissue characterisation
cellularity and fibrin mesh properties as a basis for ultrasonic tissue characterization of blood clots and thrombi (Loiacono), 399

correlations of liver echo intensity with cytology and chemical measurements of fat, water and protein content in live burbots (*Lota lota*) (Bondestam), 75

dependence of ultrasonic attenuation of liver on pathologic fat and fibrosis: examination with experimental fatty liver and liver fibrosis models (Suzuki), 657

differentiation of normal and ischemic right ventricular myocardium with quantitative two-dimensional integrated backscatter imaging (Waggoner), 249

identifying acoustic scattering sources in normal renal parenchyma *in vivo* by varying arterial and ureteral pressures (Insana), 587

in vitro classification of gallstones by quantitative echography (Goedegebure), 553

Tissue composition
correlations of liver echo intensity with cytology and chemical measurements of fat, water and protein content in live burbots (*Lota lota*) (Bondestam), 75

Tissue mimicking
temperature rise in a tissue-mimicking material generated by unfocused and focused ultrasonic transducers (Wu), 495

ultrasonic vibrational potentials in gels and preparations of biological tissue (Rosenfeld), 607

Todros, T., see Guiot, C.

Todros, T., Guiot, C. and Piantà, P. G.: modelling the feto-placental circulation: 2. A continuous approach to explain normal and abnormal flow velocity waveforms in the umbilical arteries, 545

Toikkanen, S., see Bondestam, S.

Totaro, R., Marini, C., Cannarsa, C. and Prencipe, M.: reproducibility of transcranial Dopplersonography: a validation study, 173

Transvaginal color flow imaging
the assessment of benign uterine tumor vascularization by transvaginal color Doppler (Kurjak), 645

Triphasic flow
color Doppler characteristics in normal lower extremity arteries (Hatsukami), 167

Tsuchiya, H., see Matsumoto, M.

Tumours
architectural distortion of subcutaneous fascial layer in breast tumors: ultrasonographic evaluation (Nishimura), 815

computer model of ultrasonic hyperthermia and ablation for ocular tumors using B-mode data (Lizzi), 59

Turbulence
comparison of flow disturbances in small carotid atheroma using a multi-gate pulsed Doppler system and Doppler color flow imaging (Steinke), 11

Tusé, D., see Prohaska, S. S.

U

Umbilical flow
new implanted Doppler sensors for the assessment of the main fetal hemodynamics (Arbeille), 97

Uterine artery
the assessment of benign uterine tumor vascularization by transvaginal color Doppler (Kurjak), 645

V

V79
modest enhancement of ultrasound-induced mutations in V79 cells *in vitro* (Doida), 465

Vaillant, L., see Berson, M.

Van Bel, F., Steendijk, P., Teitel, D. F., de Winter, J. P., Van der Velde, E. T. and Baan, J.: cerebral blood flow velocity: the influence of myocardial contractility on the velocity waveform of brain supplying arteries, 441

Van der Velde, E. T., see Van Bel, F.

Vascular input impedance
factors determining aortic and umbilical blood flow pulsatility in fetal sheep (Adamson), 255

Vattyam, H. M., Shu, M. C. S. and Rittgers, S. E.: quantification of Doppler color flow images from a stenosed carotid artery model, 195

Vector Doppler
vector Doppler: accurate measurement of blood velocity in two dimensions (Overbeck), 19

visualization of complex flow fields, with application to the interpretation of colour flow Doppler images (Vera), 1

Velocity flow indices
factors determining aortic and umbilical blood flow pulsatility in fetal sheep (Adamson), 255

how useful are acceleration- and deceleration-based Doppler indices? A trial on patients with percutaneous transluminal angioplasty (Windeck), 525

modelling the feto-placental circulation: 1. A distributed network predicting umbilical haemodynamics throughout pregnancy (Guiot), 535

modelling the feto-placental circulation: 2. A continuous approach to explain normal and abnormal flow velocity waveforms in the umbilical arteries (Todros), 545

new implanted Doppler sensors for the assessment of the main fetal hemodynamics (Arbeille), 97

Velocity waveforms

a method for computer simulation of ultrasound Doppler color flow images—I. Theory and numerical method (Kerr), 861

a velocity evaluation phantom for colour and pulsed Doppler instruments (Rickey), 479

factors determining aortic and umbilical blood flow pulsatility in fetal sheep (Adamson), 255

Vera, N., Steinman, D. A., Ethier, C. R., Johnston, K. W. and Cobbold, R. S. C.: visualization of complex flow fields, with application to the interpretation of colour flow Doppler images, 1

Vertebral arteries

continuous and simultaneous ultrasound Doppler velocity of the internal carotid and vertebral arteries: preliminary observations of cerebral blood flow changes with common carotid compression (Makinaga), 637

Vibration potentials

ultrasonic vibrational potentials in gels and preparations of biological tissue (Rosenfeld), 607

Vlahovich, S., see Bly, S. H. P.

Volumetric flow

comparison of flow disturbances in small carotid atheroma using a multi-gate pulsed Doppler system and Doppler color flow imaging (Steinke), 11

new implanted Doppler sensors for the assessment of the main fetal hemodynamics (Arbeille), 97

W

Waggoner, A. D., Pérez, J. E., Miller, J. G. and Sobel, B. E.: differentiation of normal and ischemic right ventricular myocardium with quantitative two-dimensional integrated backscatter imaging, 249

Walters, E., see Child, S. Z.

Waveform shape indices

how useful are acceleration- and deceleration-based Doppler indices? A trial on patients with percutaneous transluminal angioplasty (Windeck), 525

Way, J. S., see Margulies, N.

Wendling, F., Jones, S. A. and Giddens, D. P.: simulation of Doppler ultrasound signals for a laminar, pulsatile, nonuniform flow, 179

White, D. N.: the early development of neurosonology: I. Echoencephalography in adults, 115

White, D. N.: the early development of neurosonology: II. Fetal and neonatal echoencephalography, 227

White, D. N.: the early development of neurosonology: III. Pulsatile echoencephalography and Doppler techniques, 323

Wieland, W., see Steinbach, P.

Wild, S. R., see Pye, S. D.

Windeck, P., Labs, K.-H. and Jaeger, K. A.: how useful are acceleration- and deceleration-based Doppler indices? A trial on patients with percutaneous transluminal angioplasty, 525

de Winter, J. P., see Van Bel, F.

Wladimiroff, J. W., see Burghouwt, M.
Wladimiroff, J. W., see Huisman, T. W. A.
Wladimiroff, J. W., see van der Mooren, K.
Wladimiroff, J. W., see Struijk, P. C.

Wood, J. G., see Insana, M. F.

Wu, J. and Nyborg, W. L.: temperature rise generated by a focussed Gaussian beam in a two-layer medium, 293
Wu, J., Chase, J. D., Zhu, Z. and Holzapfel, T. P.: temperature rise in a tissue-mimicking material generated by unfocused and focused ultrasonic transducers, 495

X

X-ray CT
in vitro classification of gallstones by quantitative echography (Goedegebure), 553

Y

Yang, G., see Fay, B.

Yaremko, M. M., see Loiacono, L. A.

Z

Zhu, Z., see Wu, J.

Zierler, R. E., see Hatsukami, T. S.

Ziskin, M. C., see Margulies, N.

Zuna, I., see Fein, M.